



AMERICAN METEOROLOGICAL SOCIETY

Bulletin of the American Meteorological Society

EARLY ONLINE RELEASE

This is a preliminary PDF of the author-produced manuscript that has been peer-reviewed and accepted for publication. Since it is being posted so soon after acceptance, it has not yet been copyedited, formatted, or processed by AMS Publications. This preliminary version of the manuscript may be downloaded, distributed, and cited, but please be aware that there will be visual differences and possibly some content differences between this version and the final published version.

The DOI for this manuscript is doi: 10.1175/BAMS-D-17-0175.1

The final published version of this manuscript will replace the preliminary version at the above DOI once it is available.

If you would like to cite this EOR in a separate work, please use the following full citation:

Andrews, E., P. Sheridan, J. Ogren, D. Hageman, A. Jefferson, J. Wendell, A. Alastuey, L. Alados-Arboledas, M. Bergin, M. Ealo, A. Hallar, A. Hoffer, I. Kalapov, M. Keywood, J. Kim, S. Kim, F. Kolonjari, C. Labuschagne, N. Lin, A. Macdonald, O. Mayol-Bracero, I. McCubbin, M. Pandolfi, F. Reisen, S. Sharma, J. Sherman, M. Sorribas, and J. Sun, 2018: Overview of the NOAA/ESRL Federated Aerosol Network. *Bull. Amer. Meteor. Soc.* doi:10.1175/BAMS-D-17-0175.1, in press.



1 **Overview of the NOAA/ESRL Federated Aerosol Network**

2
3 Elisabeth Andrews¹, Patrick J. Sheridan², John A. Ogren², Derek Hageman¹, Anne Jefferson¹,
4 Jim Wendell², Andrés Alastuey³, Lucas Alados-Arboledas⁴, Michael Bergin⁵, Marina Ealo³, A.
5 Gannet Hallar^{6,7}, Andras Hoffer⁸, Ivo Kalapov⁹, Melita Keywood¹⁰, Jeongeun Kim¹¹, Sang-Woo
6 Kim¹², Felicia Kolonjari¹³, Casper Labuschagne¹⁴, Neng-Huei Lin¹⁵, AnneMarie Macdonald¹³,
7 Olga L. Mayol-Bracero¹⁶, Ian B. McCubbin⁷, Marco Pandolfi³, Fabienne Reisen¹⁰, Sangeeta
8 Sharma¹³, James P. Sherman¹⁷, Mar Sorribas¹⁸, Junying Sun¹⁹

9
10 ¹Cooperative Institute for Research in Environmental Sciences (CIRES), University of Colorado,
11 Boulder, CO USA

12
13 ²Earth System Research Laboratory (ESRL), National Oceanic and Atmospheric Administration
14 (NOAA), Boulder, CO USA

15
16 ³Institute of Environmental Assessment and Water Research, Barcelona, Spain

17
18 ⁴Andalusian Institute for Earth System Research, IISTA-CEAMA, University of Granada,
19 Granada, Spain

20
21 ⁵Department of Civil & Environmental Engineering, Duke University, Durham, NC, USA

22
23 ⁶University of Utah, Department of Atmospheric Science, Salt Lake City, UT, USA

24

25 ⁷Storm Peak Laboratory, Desert Research Institute, Steamboat Springs, CO, USA

26

27 ⁸MTA-PE Air Chemistry Research Group, University of Pannonia, Veszprém, Hungary

28

29 ⁹Institute for Nuclear Research and Nuclear Energy, Basic Environmental Observatory

30 Moussala, Sofia, Bulgaria

31

32 ¹⁰CSIRO Oceans and Atmosphere, Aspendale, Australia

33

34 ¹¹Environmental Meteorology Research Division, National Institute of Meteorological Sciences

35 (NIMS), Seogwipo-si, Jeju-do, R. Korea

36

37 ¹²School of Earth and Environmental Sciences, Seoul National University, Seoul, Korea

38

39 ¹³Environment and Climate Change Canada, Toronto, Ontario, Canada

40

41 ¹⁴Climate Environmental Research Monitoring (CERM), South African Weather Service,

42 Stellenbosch, South Africa

43

44 ¹⁵Department of Atmospheric Sciences, National Central University, Taoyuan, Taiwan

45

46 ¹⁶Department of Environmental Science, University of Puerto Rico - Rio Piedras, San Juan,
47 Puerto Rico, USA

48

49 ¹⁷Department of Physics and Astronomy, Appalachian State University, Boone, NC, USA

50

51 ¹⁸El Arenosillo Atmospheric Sounding Station, Atmospheric Research and Instrumentation
52 Branch, National Institute for Aerospace Technology (INTA), Huelva, Spain

53

54 ¹⁹State Key Laboratory of Severe Weather & Key Laboratory of Atmospheric Chemistry of
55 CMA, Chinese Academy of Meteorological Sciences, Beijing, Peoples Republic of China

56

57 Corresponding author: Elisabeth Andrews,

58 Email: betsy.andrews@noaa.gov

59 Address: NOAA/ESRL/GMD, 325 Broadway, Boulder, CO 80305, USA

60 Phone: 303-497-5171

61

62 **Overview of the NOAA/ESRL Federated Aerosol Network**

63

64 **Capsule**

65 The cooperative nature of NOAA's Federated Aerosol Network allows for collection of
66 consistent datasets for evaluating regionally representative aerosol climatologies, trends, and
67 radiative forcing at 30 sites around the world.

68

69 **Abstract**

70 In order to estimate global aerosol radiative forcing, measurements of aerosol optical properties
71 are made by the NOAA Earth System Research Laboratory's Global Monitoring Division
72 (ESRL/GMD) and their collaborators at 30 monitoring locations around the world. Many of the
73 sites are located in regions influenced by specific aerosol types (e.g., Asian and Saharan desert
74 dust, Asian pollution, biomass burning, etc.). This network of monitoring stations is a shared
75 endeavor of NOAA and many collaborating organizations, including the World Meteorological
76 Organization Global Atmosphere Watch (WMO/GAW) Program, the U.S. Department of Energy
77 (DOE), several U.S. and foreign universities, and foreign science organizations. The result is a
78 long-term, cooperative program making atmospheric measurements that are directly comparable
79 with those from all the other network stations and with shared data access. The protocols and
80 software developed to support the program facilitate participation in GAW's atmospheric
81 observation strategy and the sites in the NOAA/ESRL network make up a substantial subset of
82 the GAW aerosol observations. This paper describes the history of the NOAA/ESRL Federated
83 Aerosol Network, details about measurements and operations and some recent findings from the
84 network measurements.

85

86 **1. Introduction**

87 Climate change is one of the most important environmental, social, economic, and political
88 issues facing the planet today. Aerosol particles may have either a warming or cooling effect at
89 the top-of-atmosphere, depending both on properties of the aerosol and the underlying surface
90 (IPCC, 2013). Atmospheric aerosol particles interact with solar radiation by absorbing and
91 scattering light. The amount of scattering and absorption is a function of particle size,
92 composition, and shape, as well as external variables like relative humidity (RH) and wavelength
93 of incident light. The regional influence of aerosol particles on climate and weather tends to be
94 stronger than their global average impact, due to their relatively short atmospheric lifetimes and
95 inhomogeneity in sources and processing. Thus, to understand the global influence of aerosol
96 particles, it is necessary to make long-term measurements at many regionally representative sites
97 (e.g., Laj et al., 2009; Lund Myhre and Baltensperger, 2012). Short-term aerosol campaign
98 measurements are typically designed to study specific processes and/or events, but long-term
99 measurements are often needed to put such data into a broader context, e.g., to assess whether
100 field campaign measurements represent that location and season, as well as for assessing trends
101 and variability. Such long-term measurements can take the form of ground-based remote
102 sensing, satellite-based remote sensing, and/or ground-based in-situ sites. While the focus here
103 is on long-term, surface in-situ sites, it is important to recognize the synergy obtained when data
104 from multiple independent platforms are combined (e.g., Ogren, 1995; Kahn et al., 2004, 2017;
105 Anderson et al., 2005). For example, combining surface measurements with airborne or remote
106 sensing platforms enables the connection of ground-based aerosol properties to vertically-
107 resolved processes. While ground-based, in-situ measurements cannot represent the properties

108 of aerosols that are present in layers aloft, multi-year in-situ aerosol profiling measurements over
109 two FAN sites in the US have shown that ground-based measurements of aerosol intensive
110 properties such as single scattering albedo and scattering Ångström exponent can represent the
111 climatology of those properties aloft under well-mixed conditions (Andrews et al., 2004;
112 Sheridan et al., 2012).

113
114 Numerous stations around the world make long-term in-situ measurements of regionally-
115 representative aerosol optical properties. Originally, many of these sites were operated in
116 isolation to address specific scientific goals with sampling and data protocols designed to meet
117 those goals, making it difficult to utilize those data in wider studies and inter-comparisons
118 (Kulmala et al., 2011). Several recent papers note the importance of consistent operational and
119 data processing among sites in order to improve data quality control and access across locations
120 (e.g., Kulmala et al., 2011; Wiedensohler et al., 2012). In contrast, some sites (e.g., the original
121 NOAA Baseline Observatories, Bodhaine, 1983) were conceived as part of a network where
122 similarities in instruments, protocols, and a common data archive resulted in complete intra-
123 network consistency, although extra-network comparisons were limited by differences in data
124 collection and/or treatment. Recognition of the need for consistent measurements drives the
125 development of protocols for instruments and data treatment (e.g., WMO, 2016).

126
127 This paper presents a description of the current NOAA Federated Aerosol Network (FAN),
128 which evolved from the original NOAA baseline network. The two primary purposes of this
129 paper are (1) to describe the current state of the FAN (including its member stations, the
130 measurements common to most of the stations, and the sampling and measurement protocols)

131 and (2) to show examples of the science that is possible with a global network of this type. A
132 number of earlier papers (e.g., Sheridan et al., 2001; Delene and Ogren, 2002; Sherman et al.,
133 2015) touched on some aspects of this, utilizing small subsets of the network (1 to 4 stations)
134 but, until now, there have been no papers describing the FAN in its entirety. The paper begins
135 with a brief history of the network, discusses the key measurements and measurement protocols
136 made at network sites, describes the software for data acquisition and processing, and finally,
137 presents an overview of scientific results from FAN measurements over the last 15 years.

138

139 **2. History of the NOAA Federated Aerosol Network**

140 The current network mission is to characterize the means, variability, and trends of climate-
141 forcing properties of different types of aerosols, and to understand the factors that control these
142 properties. In the 1970s, NOAA's Environmental Research Laboratories (ERL) Geophysical
143 Monitoring for Climatic Change (GMCC) Program had the mission to detect changes (i.e.,
144 trends, cycles) in the long-term global aerosol background values. To do so, GMCC conducted
145 aerosol measurements at four baseline observatories. The original NOAA Baseline
146 Observatories (Mauna Loa, Hawaii (MLO), the South Pole (SPO), American Samoa (SMO), and
147 Barrow, Alaska (BRW)) appear along the left-hand side of Figure 1. These sites are remote from
148 aerosol sources and typically represent clean background air, although, occasionally, they may
149 be impacted by long range transport (e.g., Perry et al., 1999; Stone et al., 2007).

150

151 Since the initial founding of the baseline observatory network, the scientific understanding of the
152 properties and impacts of atmospheric aerosols has improved considerably. In response to the
153 finding that anthropogenic aerosols create a significant perturbation in the Earth's radiative

154 balance on regional scales (e.g., Bolin and Rodhe, 1976; Charlson et al., 1991), NOAA expanded
155 its aerosol research program starting in 1992 to include four sites in North America: Bondville,
156 Illinois (BND, collaboration with University of Illinois), Sable Island, Nova Scotia (WSA,
157 collaboration with Environment and Climate Change Canada), Southern Great Plains (SGP,
158 collaboration with US Department of Energy)) and Trinidad Head, California (THD). These site
159 locations were chosen because they are at times impacted by anthropogenic aerosols and
160 consequently address the need to better understand how human activity can influence the
161 radiation balance. Although these sites are not as remote as the baseline observatories, they also
162 are not close to major anthropogenic aerosol sources (e.g., Delene and Ogren, 2002) and
163 typically provide measurements of regionally representative aerosol (e.g., Wang et al., 2018).

164

165 ESRL/GMD's expertise in maintaining long-term measurements of aerosol optical properties
166 (often at remote locales) did not go unnoticed. Colleagues from around the world contacted
167 GMD for advice on station operations and instrument maintenance and the collaborative
168 NOAA/ESRL Federated Aerosol Network was born. The concept for and, indeed, the name of
169 the FAN, owes much to the development of the AERONET sunphotometer network in the mid-
170 1990s (Holben et al., 1998). The definition of a federation is groups "*that have joined together*
171 *for a common purpose*" (Collins, 2018). The descriptor 'federated' is appropriate as the result is
172 a long-term, cooperative program with shared data access making atmospheric measurements
173 that are directly comparable with all the other FAN stations. FAN collaborators contribute
174 scientific interest, instruments, onsite technicians, long-term station costs, and operations support
175 while NOAA contributes software for data acquisition and processing, as well as technical
176 expertise. It is a true partnership where both sides are learning from each other. A major

177 advantage is that the NOAA software and protocols streamline data acquisition and processing
178 (discussed below) so that more time can be spent on science. Since 2010, more than 50 papers
179 using FAN network data have been published (NOAA, 2018a) and multiple graduate theses have
180 also been submitted. FAN support has also improved data submission to the World Data Center
181 for Aerosols (www.gaw-wdca.org), both in terms of quantity of data submitted and quality and
182 completeness of the submitted data sets.

183

184 Since 2004, 25 sites operated by numerous collaborators have joined FAN (prior to 2004 only six
185 sites were in the network – NOAA’s four baseline observatories and 2 regional stations running
186 NOAA instruments and supervised by NOAA scientists). Many of these new cooperative aerosol
187 monitoring sites are situated in regions where significant aerosol forcing is anticipated, including
188 locations in North America, Europe, and Asia. Figure 1 illustrates that, while there is reasonable
189 global coverage, there are also some large spatial gaps (particularly in the southern hemisphere)
190 due to finite funding resources and limited infrastructure as well as the lack of collaborators in
191 those regions. NOAA has as major partners in these global and regional aerosol measurements
192 the World Meteorological Organization Global Atmosphere Watch (WMO/GAW) Program, and
193 several US and foreign universities and science agencies. Most of the collaborative stations are
194 run under the auspices of the GAW network, thus FAN sites may be considered a substantial
195 subset of the larger GAW surface in-situ aerosol monitoring network. (FAN data comprises
196 approximately 1/3 of GAW’s surface aerosol optical property measurements and dominates
197 contributions of optical properties to GAW outside of Europe). Table S1 provides more detail
198 about the sites shown in Figure 1.

199

200 **3. Description of system**

201 The basic aerosol optical property measurements made at FAN sites are spectral aerosol light
202 scattering (total and backwards hemisphere) and light absorption. These are the critical
203 parameters for determining aerosol direct radiative forcing. Most of the sites also measure
204 aerosol number concentration. Depending on the station, additional aerosol and gas-phase
205 measurements may be available. Over the years, NOAA/GMD has developed protocols and
206 instrument infrastructure in order to make measurements of known, high quality and has written
207 software to enable consistent processing, editing, and archiving of the data. NOAA (2018b)
208 provides details, design drawings and photos of the system components (inlet, instruments,
209 auxiliary control units, pumpbox, etc.), but brief descriptions of the main components are
210 provided below.

211

212 **3.1 Instruments**

213 Light scattering by atmospheric aerosols at the FAN stations is measured using integrating
214 nephelometers (currently, either the TSI (model 3563, TSI Inc., St Paul, MN) or the Ecotech
215 (Aurora 3000/4000, Ecotech, Melbourne, Australia) nephelometer). Both instruments measure
216 total and hemispheric aerosol back-scattering coefficients at three visible wavelengths, enabling
217 calculation of spectral aerosol properties and various proxies describing the angular distribution
218 of light scattering (e.g., Andrews et al., 2006). Table S1 describes the scattering and absorption
219 instruments at each site. Table S2 in the supplemental materials gives further details (e.g.,
220 wavelengths) for the various instruments.

221

222 Aerosol light absorption is measured at FAN stations using a variety of filter-based absorption
223 instruments. Currently, the primary light absorption instruments are the ESRL/GMD-developed

224 three-wavelength Continuous Light Absorption Photometer (CLAP, Ogren et al., 2017) and the
225 single-wavelength Multi-Angle Absorption Photometer (MAAP, Thermo Fisher Scientific,
226 Franklin, MA). Many sites are also operating 7-wavelength aethalometers (Magee Scientific,
227 Berkeley, CA) to take advantage of that instrument's broad spectral range. Previously, FAN
228 sites used single- and multi-wavelength Particle Soot Absorption Photometers (PSAP, Radiance
229 Research Inc., Seattle, WA) and/or broadband aethalometers.

230

231 While the instruments across the FAN are not identical, laboratory studies suggest they make
232 comparable measurements. Intercomparisons of TSI and Ecotech nephelometers show excellent
233 reproducibility for total scattering although the differences are slightly larger for backscattering
234 (Mueller et al., 2011b). Mueller et al. (2011a) find good between PSAP and MAAP
235 measurements of aerosol light absorption for a 2007 intercomparison study although less
236 agreement existed for an earlier (2005) data set. Mueller et al (2011a) also identify a fairly wide
237 range of variability in PSAPs, but show much of the variability was due to spot size variations
238 and flow rate issues. The PSAPs and CLAPs in the FAN are corrected for spot size and operated
239 at a consistent flow rate (face velocity of 0.8 m/s) to minimize these issues. Ogren et al. (2017)
240 demonstrate excellent agreement between long-term measurements with PSAPs and CLAPs at
241 multiple sites in the FAN. Sherman et al. (2015) present measurement uncertainties for
242 scattering and absorption measurements as well as for calculated parameters such as single
243 scattering albedo and Ångström exponent.

244

245 Aerosol number concentration is another common measurement at FAN sites (Table S3). The
246 most commonly used instruments for this parameter are butanol-based particle counters. Many

247 FAN sites operate multiple particle counters in tandem which can provide some minimal
248 information on aerosol size distribution because different models have different lower size cuts.
249 Some sites also operate instruments to measure aerosol size distributions (see Table S3).

250

251 **3.2 Infrastructure and Protocols**

252 The FAN is a subset of the WMO Global Atmosphere Watch, and consequently follows the
253 GAW aerosol guidelines and standard operating procedures (WMO, 2011; 2016). The WMO
254 World Calibration Center for Aerosol Physics (WCCAP, 2018) organizes instrument training and
255 evaluation workshops and performs occasional site audits that are designed to ensure consistency
256 across the GAW network. The role of FAN, in this context, is to provide advice and tools that
257 make it easier for stations operators to implement the recommended procedures for GAW
258 stations.

259

260 The FAN standard aerosol inlet configuration (NOAA, 2018c) is slightly anisokinetic (i.e.,
261 Reynolds number in the range 4500-7000). The resulting turbulent conditions limit losses of
262 super micrometer particles (Wilcox, 1956). Sampling line sizes, materials, pickoffs, and flow
263 rates are optimized to promote maximum passing efficiency for particles that are most important
264 to radiative forcing (i.e., particles with diameters between 0.1 and 10 μm). Because the focus is
265 primarily on optically important aerosol, bends in tubing and obstructions upstream of
266 instruments are minimized to limit particle losses due to impaction. Passing efficiencies for
267 super-micron particles are 99% and 50% for 1-2 and 7-11 μm aerodynamic diameter particles,
268 respectively. Different inlet designs and/or instruments should be used for aerosol diameters
269 above this size range. The inlet is not optimized for ultrafine aerosol, however inlet passing

270 efficiency calculations suggest a 99% and 50% passing efficiency for 0.1 and 0.002-0.004 μm
271 aerodynamic diameter particles, respectively. Figure S1 in supplemental materials shows the
272 aerosol inlet passing efficiency for several stations. Some collaborators have designed their own
273 inlet system (see Table S3). The GAW report 227 (WMO, 2016) includes guidelines for inlet
274 systems, including criteria and equations used to design them. GAW and FAN offer assistance to
275 station operators to design inlet systems and calculate losses, but every site is different (e.g.,
276 surrounding terrain and vegetation, fog frequency) meaning a common design is not practical or
277 even desirable.

278
279 The network goal is to make aerosol measurements at low relative humidity ($\text{RH} < 40\%$) which
280 minimizes the confounding effects of aerosol amount and hygroscopicity on the optical
281 properties, facilitating comparison of aerosol properties among FAN sites. This objective is
282 consistent with the wider GAW sampling protocol (WMO, 2016). To achieve low RH, two
283 approaches have been used. The first involves gentle heating (to a maximum of 40°C) of the
284 sample lines and insulation of the sample lines downstream of the heater. Power is only applied
285 to the heater when the sample humidity is above the desired value. The second approach is to
286 dilute the air stream with dry, filtered air generated by a compressor system. The dilution
287 approach is typically used at warm marine sites in the network. The amount of dilution air is
288 measured and corrections to the measurements are applied automatically during data processing.

289
290 In order to fully characterize the sampling system, temperature, RH, flow, and pressure are
291 monitored at several points along the sample line. Monitoring temperature and RH in several
292 places allows determination of whether sample dewpoint temperature is maintained as the air

293 moves through the system. Discrepancies in system dewpoint temperature can indicate a leak in
294 the system (or, possibly, a poorly calibrated sensor). Pressure and flow measurements provide
295 diagnostics to determine whether sample air is flowing through the system as designed.
296 Additionally, both analog and digital flow and pressure measurements are implemented. The
297 analog measurements (e.g., rotameters, pressure gauges, etc.) can be assessed at a glance by an
298 on-site operator. The digital measurements are also available to the on-site operator via the data
299 acquisition interface, but are primarily intended for someone who is remotely evaluating the
300 data.

301
302 Many FAN sites make aerosol light scattering and absorption coefficient measurements at two
303 size cuts (aerodynamic particle diameter <1 and <10 μm (PM1 and PM10)). ESRL/GMD has
304 designed an ‘impactor box’ to smoothly integrate size cut switching into system operations. All
305 sample air flows through a 10 μm multi-jet Berner impactor (Hillamo and Kauppinen, 1991 and
306 references therein) prior to being sampled by instruments. On a time base interval ranging from
307 5 min to 30 min, depending on the site, control software closes an automated ball valve, forcing
308 the sample flow through a 1 μm Berner impactor. A mass flow controller is used to control flow
309 through the impactors in order to ensure the desired size cut. The impactor box also contains
310 solenoid valves that enable the instruments to be bypassed at certain times (e.g., during impactor
311 cleaning).

312
313 The system requires only minor intervention from on-site technicians. Technician tasks include
314 nephelometer calibration gas checks (performed with CO₂ and filtered air) to verify instrument
315 calibration (Anderson and Ogren, 1998); impactor cleaning; filter changes for the light

316 absorption instruments; and replenishing the operating fluid for number concentration
317 instruments. The frequency of these tasks depends on the site. Most sites perform nephelometer
318 calibration checks and impactor servicing on a weekly to monthly basis, while filter changes and
319 operating fluid replenishment tend to be more frequent. Figure S2 provides an example of
320 nephelometer calibration checks for FAN sites with at least 5 years of data. Annually, or
321 whenever problems are suspected, FAN protocols recommend calibration of system sensors (T,
322 P, RH, flow), cleaning of instruments and sample lines, and overnight filtered air tests on
323 scattering and absorption instruments.

324

325 It should be noted that there is currently no calibration standard for filter-based absorption
326 measurements (that is an area of active research, e.g., EMPIRBlackCarbon (2018)) but the flows
327 for the absorption instruments are calibrated annually. NOAA/GMD does not utilize a
328 calibration system for particle counters, however, two particle counters are maintained as
329 reference standards, one of which was tested at the WCCAP for connecting the FAN
330 measurements with the wider GAW network. Field CPCs are periodically tested against these
331 lab reference CPCs. The CPC flows are also checked on a regular basis. Instrument
332 intercomparisons are a major tool in the in-situ aerosol community for ensuring comparable
333 measurements, due to the lack of calibration standards. Additionally, instrument noise
334 evaluations are performed annually for scattering, absorption and number concentration
335 instruments; these evaluations consist of having the instruments measure filtered air for a 12-24 h
336 period.

337

338 **3.3 Software**

339 ESRL/GMD has developed custom software (called CPD3) for acquisition, processing, editing
340 and archiving of data from aerosol instruments that are used in the FAN. More information about
341 the software is available in supplemental materials but some key aspects are highlighted here.
342 An earlier version of the ESRL/GMD software (CPD2) is also used in the CATCOS aerosol
343 network (Capacity Building and Twinning for Climate Observing Systems, PSI (2018)). The
344 same software suite is used for both field acquisition computers and offsite data processing and
345 analysis. Scientists and technicians responsible for the data use another copy of CPD3 on their
346 desktop or laptop computers to review the data for quality and completeness and flag or remove
347 contaminated or invalid data. The CPD3 system supports direct submission of both near real-
348 time (raw data) and annual (QC-reviewed) data to the WMO World Data Center for Aerosols.
349
350 CPD3 is highly configurable, making it simple to add or remove instruments at the field site and
351 to change data logging parameters. A list of instruments that can be logged with CPD3 is
352 available from NOAA (2018d). Because all instruments are logged on the same computer using
353 the time server synched computer timestamp, the timestamp for every instrument is the same.
354 Having all the instruments and infrastructure tied together enables the system to operate
355 holistically. For example, if high particle concentrations and/or wind direction indicate local
356 contamination can flagged automatically (e.g., Sheridan et al., 2016). Similarly, chemical filters
357 can be automatically bypassed to avoid sampling contaminated air while other measurements are
358 flagged (Quinn et al., 2002).
359
360 During data review, the ability to inspect multiple data streams simultaneously in a graphical
361 interface helps both with identifying events and troubleshooting system failures. CPD3 includes

362 a time-stamped message log enabling the data to be directly related to operator actions and
363 observations both on the station computer and after the fact during quality control (QC) data
364 inspection and editing. CPD3 provides tools for editing and applying standard corrections (e.g.,
365 standard temperature and pressure corrections, the truncation correction for the nephelometer
366 (Anderson and Ogren 1998), various schemes for correcting filter-based absorption
367 measurements (e.g., Bond et al., 1999), etc. The end result of the integrated software developed
368 at ESRL/GMD is a self-consistent data archive standardized across all stations using the
369 software. Final data from the NOAA/ESRL FAN are available from the WDCA (NILU, 2018)
370 for most stations and from the PIs in all cases.

371

372 **4. FAN science**

373 While the FAN methodology is useful for a single station, its real strength lies in creating
374 measurement consistency amongst multiple stations. Science questions that can be addressed
375 with this data set include:

- 376 • What are the range and variability (on multiple time scales) of aerosol optical properties
377 observed at FAN sites?
- 378 • How do long-term trends in aerosol properties compare across the globe?

379

380 By combining FAN data with external data sets, additional questions can be explored:

- 381 • Can similarities and differences among sites be related to aerosol types, sources, or
382 processes?
- 383 • How well do global models and aerosol parameterizations in models capture aerosol
384 properties across a range of sites?

- 385 • How consistent are the in-situ aerosol properties measured at FAN sites with remote-
386 sensing measurements from ground- and satellite-based instruments, and how do the
387 consistencies and inconsistencies inform interpretation of the results from all three
388 approaches?

389
390 Figure 2 illustrates that the FAN sites cover a wide range of aerosol properties. Aerosol loading
391 (e.g., scattering and absorption) spans nearly four orders of magnitude. While scattering at the
392 sites is shown in monotonically increasing order, other aerosol parameters (e.g., single-scattering
393 albedo and scattering Ångström exponent, see Table 1) vary as a function of the nature of the
394 particles (e.g., size, composition) rather than aerosol amount. For example, the clean marine
395 sites (Cape Grim, Australia (CGO), Cape Point, South Africa (CPT), American Samoa (SMO),
396 Trinidad Head, CA (THD) and Cape San Juan, PR (CPR)) exhibit low scattering Ångström
397 exponent (SAE) values indicative of large sea salt aerosol, while the low SAE at Mount
398 Waliguan, China (WLG) can be attributed to large dust particles. Median single-scattering
399 albedo (SSA) values are around 0.92 at most sites, although the clean marine sites exhibit higher
400 SSA values due to predominantly white sea salt aerosol. In contrast, UGR exhibits significantly
401 lower SSA relative to the other sites in the FAN network – the site is strongly impacted by
402 diesel-based traffic and local biomass burning (Titos et al., 2017). The standardized FAN
403 sampling and data processing protocols help ensure that the reported differences between stations
404 are real and not related to operational inconsistencies. Table S1 in the supplemental materials
405 provides more information about the stations and measurement data depicted in Figure 2. Figure
406 S3 in supplemental materials shows the same data depicted in Figure 2 in separate sets of panes
407 with aerosol scattering coefficient ordered by (a) elevation, (b) latitude and (c) longitude.

408

409 While Figure 2 shows annual climatological values for all sites in the network, more detailed
410 climatologies can be evaluated as well. Figure 3 shows climatological patterns of aerosol light
411 scattering at Bondville, IL as a function of year, month and day of year. Figure 3a shows that
412 there has been a decrease in aerosol light scattering at Bondville since the start of measurements
413 in the mid-1990s and that this decrease appears to have impacted scattering during all months at
414 the site. This result is consistent with other literature documenting decreases in aerosol loading
415 over most of the continental U.S. (e.g., Collaud Coen et al., 2013). Although aerosol amounts
416 have decreased over the last two decades, the general picture of higher scattering during the
417 summer remains true. Figure 3b depicts how the diurnal cycle varies with time of year. In the
418 summer, the scattering is high throughout the day, while at other times of year the diurnal cycle
419 is much more pronounced (similar to the observations of Sherman et al. (2015)). The diurnal
420 minimum occurs in the early afternoon, most likely due to an increase in boundary layer height.

421

422 Detailed multi-site climatologies, including data from FAN observatories, based on location
423 (e.g., mountain sites (Andrews et al., 2011); North American sites (e.g., Sherman et al., 2015;
424 Delene and Ogren, 2002); and Arctic sites (Schmeisser et al., 2018)) have been published. Sites
425 in the FAN are often members of other networks (e.g., ACTRIS, 2018; IASOA, 2018) and are
426 included in reports on their climatologies as well (e.g., Uttal et al., 2016; Zanatta et al., 2016;
427 Pandolfi et al., 2018). Additionally, with multiple sites one can look at the co-variability of
428 different aerosol properties and start to identify relationships as a function of site and aerosol
429 type (e.g., Delene and Ogren, 2002; Andrews et al., 2011; Sherman et al., 2015; Schmeisser et
430 al., 2017). Trend studies have also used data from multiple FAN sites as the focus of their

431 investigation (e.g., Asmi et al., 2013; Collaud Coen et al., 2013; Sherman et al., 2015) to explore
432 changes in aerosol properties as a function of location.

433

434 An additional advantage of the unified FAN data set is that it can be used to assess and improve
435 global models. Multiple studies use FAN number concentration data to evaluate various
436 parameterizations of aerosol nucleation (e.g., Spracklen et al., 2010; Matsui et al., 2013; Mann et
437 al., 2014; Yu et al., 2014). Skeie et al. (2011) evaluated how well the Oslo CTM2 model
438 simulated absorbing aerosol in terms of loading and seasonality at multiple FAN stations. There
439 are several modeling studies using Arctic sites FAN data. For example, Sharma et al. (2013)
440 explored the sensitivity of absorbing aerosol to wet and dry deposition, while Eckhardt et al.
441 (2015) used Arctic surface measurements to evaluate simulated model climatologies. Currently,
442 the FAN data are being utilized to evaluate AEROCOM (Kinne et al., 2006) global model
443 simulations of surface aerosol scattering and absorption coefficients (Andrews et al., in
444 preparation, 2018).

445

446 While the FAN data consistency allows for collective science using data from multiple sites, the
447 unique locations and interests of scientists involved with each site have also resulted in many
448 findings. For example, there have been both climatological and transport event-based studies
449 focused on aerosol types observed at individual sites (e.g., Lim et al., 2012; Hallar et al., 2015;
450 Sorribas et al., 2015; 2017; Denjean et al., 2016; Rivera et al., 2017; Kassianov et al., 2017).
451 FAN measurements have been used to provide context for field campaigns (e.g., Brock et al.,
452 2011; Bravo-Aranda et al., 2015; Denjean et al., 2016), instrument comparisons (e.g., Sharma
453 and Barnes, 2016; Backman et al., 2017; Sinha et al., 2017; Sharma et al., 2017); remote sensing

454 validation (e.g., Pahlow et al., 2006; Di Pierro et al., 2013; Shinozuka et al., 2015)); aerosol
455 direct radiative forcing sensitivities and uncertainties (e.g. Sherman and McComiskey, 2018),
456 and many other scientific efforts.

457
458 Uniting observatories under the umbrella of the Federated Aerosol Network provides the
459 opportunity to both train and learn from a diverse group of US and international partners. The
460 federated nature of the network enables scientists to pursue their own interests while
461 participating in a wider goal, making the network greater than sum of its individual parts. In the
462 process of increasing understanding of the range and variability in aerosol radiative properties,
463 the FAN strengthens scientific ties across the globe, fostering collaborations and the exchange of
464 knowledge. In the FAN's next 25 years, the objective is to maintain current collaborations and
465 to establish new ones to expand the network, particularly in under-sampled regions. The FAN
466 will continue to improve measurements, software and protocols in order to be able to address
467 new questions as they arise. For example, in the future, a complementary network comprised of
468 new, low-cost sensors could be developed or even used to expand the FAN or other networks
469 pending guidance from WMO/GAW (e.g., WMO, 2018).

470

471 **5. Conclusions**

472 The FAN is a long-term, cooperative program enabling diverse sites with a wide range of aerosol
473 types to make measurements that are directly comparable with other network stations. This
474 facilitates the exploration of science questions at local, regional, and global scales and makes the
475 network measurements especially useful for global model evaluation. There is a need to expand
476 such measurements to locations that have large impacts by aerosols but little current

477 representation in measurement databases, but of course many factors (e.g., funding) will
478 determine whether this really takes place. The growth and scope of NOAA's collaborative
479 network can be a model for new and existing networks which seek to expand coverage in a
480 collaborative fashion.

481

482 **Acknowledgements**

483 The writing of this manuscript was supported by NOAA Climate Program Office's Atmospheric
484 Chemistry, Carbon Cycle and Climate (AC4) program. The FAN network would not be possible
485 without the interest and support of our collaborators and their students and/or technicians who
486 maintain the stations and instruments, and keep the data flowing from their observatories.

487

488

489 **References**

490 ACTRIS, 2018: Research Infrastructure for the observation of Aerosol, Clouds, and Trace gases.

491 Accessed 21 May 2018, <https://www.actris.eu/>.

492

493 Anderson, T.L., and Coauthors, 2005: An “A-Train” Strategy for Quantifying Direct Climate

494 Forcing by Anthropogenic Aerosols. *Bull. Amer. Meteor. Soc.*, **86**, 1795-1809,

495 <https://doi.org/10.1175/BAMS-86-12-1795>.

496

497 Anderson, T.L. and Ogren, J.A., 1998: Determining aerosol radiative properties using the TSI

498 3563 integrating nephelometer, *Aerosol Sci. Tech.*, **29**, 57-69, doi:10.1080/02786829808965551.

499

500 Andrews, E., and Coauthors, 2018: Comparison of aerosol optical property climatology from in-

501 situ observations and global climate model simulations, in preparation.

502

503 Andrews, E., and Coauthors, 2011: Climatology of aerosol radiative properties in the free

504 troposphere, *Atmos. Res.*, **102**, 365-393, <https://doi.org/10.1016/j.atmosres.2011.08.017>.

505

506 Andrews, E., and Coauthors, 2006: Comparison of methods for deriving aerosol asymmetry

507 parameter, *J. Geophys. Res.*, **111**, doi:10.1029/2004JD005734.

508

509 Andrews, E., Sheridan, P. J., Ogren, J. A., and Ferrare, R., 2004: In situ aerosol profiles over the

510 Southern Great Plains cloud and radiation testbed site: 1. Aerosol optical properties, *J. Geophys.*

511 *Res.*, 109, D06208, doi:10.1029/2003JD004025.

512

513 Asmi, A., and Coauthors, 2013: Aerosol decadal trends – Part 2: In-situ aerosol particle number
514 concentrations at GAW and ACTRIS stations, *Atmos. Chem. Phys.*, **13**, 895-916,
515 <https://doi.org/10.5194/acp-13-895-2013>.

516

517 Backman, J. and Coauthors, 2016: On Aethalometer measurement uncertainties and multiple
518 scattering enhancement in the Arctic, *Atmos. Meas. Tech.*, accepted,
519 <https://doi.org/10.5194/amt-2016-294>.

520

521 Bodhaine, B. A., 1983: Aerosol measurements at four background sites, *J. Geophys. Res.*, **88**,
522 10753–10768, doi:10.1029/JC088iC15p10753.

523

524 Bolin, B. and Charlson, R.J., 1976: On the role of the tropospheric sulfur cycle in the shortwave
525 radiative climate of the Earth, *Ambio*, **3**, 47-54.

526

527 Bond, T. C., Anderson, T. L., and Campbell, D., 1999: Calibration and intercomparison of filter-
528 based measurements of visible light absorption by aerosols, *Aerosol Sci. Technol.*, **30**, 582–600,
529 doi:10.1080/027868299304435.

530

531 Bravo-Aranda, J.A. and Coauthors, 2015: Study of mineral dust entrainment in the planetary
532 boundary layer by lidar depolarisation technique, *Tellus B*, **67**, 26180, doi:
533 10.3402/tellusb.v67.26180.

534

535 Brock, C.A. and Coauthors, 2011: Characteristics, sources, and transport of aerosols measured in
536 spring 2008 during the aerosol, radiation, and cloud processes affecting Arctic Climate
537 (ARCPAC) Project, *Atmos. Chem. Phys.*, **11**, 2423-2453,
538 <https://doi.org/10.5194/acp-11-2423-2011>.
539
540 Charlson, R.J., Langner, J., Rodhe, H., Leovy, C.B., and Warren, S.G., 1991: Perturbation of the
541 northern hemisphere radiative balance by backscattering from anthropogenic sulfate aerosols,
542 *Tellus*, **43AB**, 152-163, doi:10.1034/j.1600-0870.1991.00013.x.
543
544 Collaud Coen, M., and Coauthors, 2013: Aerosol decadal trends – Part 1: In-situ optical
545 measurements at GAW and IMPROVE stations, *Atmos. Chem. Phys.*, **13**, 869-894,
546 <https://doi.org/10.5194/acp-13-869-2013>.
547
548 Collins., 2018: Definition of 'federated'. Accessed 21 May 2018,
549 <https://www.collinsdictionary.com/us/dictionary/english/federated>
550
551 Delene, D. J. and Ogren, J. A., 2002: Variability of aerosol optical properties at four North
552 American surface monitoring sites, *J. Atmos. Sci.*, **59**, 1135–1150, doi:10.1175/1520-
553 0469(2002)059<1135:VOAOPA>2.0.CO;2.
554
555 Denjean, C. and Coauthors, 2016: Size distribution and optical properties of African mineral dust
556 after intercontinental transport, *J. Geophys. Res.*, **121**, 7117-7138, doi:10.1002/2016JD024783.
557

558 Di Pierro, M., Jaegle, L., Eloranta, E.W., Sharma, S., 2013: Spatial and seasonal distribution of
559 Arctic aerosols observed by the CALIOP satellite instrument (2006–2012), *Atmos. Chem. Phys.*,
560 **13**, 13, 7075-7095, <https://doi.org/10.5194/acp-13-7075-2013>.
561

562 Eckhardt, S. and Coauthors, 2015: Current model capabilities for simulating black carbon and
563 sulfate concentrations in the Arctic atmosphere: a multi-model evaluation using a comprehensive
564 measurement data set, *Atmos. Chem, Phys.*, **15**, 9413–9433, doi:10.5194/acp-15-9413-2015.
565

566 EMPIRBlackCarbon, 2018: Black Carbon Metrology for light absorption by atmospheric
567 aerosols. Accessed 21 May 2018, <http://www.empirblackcarbon.com>.
568

569 Hallar, A.G., Petersen, R., Andrews, E., Michalsky, J., McCubbin, I., Ogren, J.A., 2015:
570 Contributions of dust and biomass-burning to aerosols at a Colorado mountain-top site, *Atmos.*
571 *Chem. Phys.*, **15**, 13665-13679, <https://doi.org/10.5194/acp-15-13665-2015>.
572

573 Hillamo, R.E. and Kauppinen, E.I, 1991: On the performance of the Berner low pressure
574 impactor, *Aerosol Sci. Technol.*, **14**, 33-47, doi: 10.1080/02786829108959469.
575

576 Holben, B.N. and Coauthors, 1998: AERONET - A federated instrument network and data
577 archive for aerosol characterization. *Remote Sensing of Environment*, **66**, 1-16,
578 [https://doi.org/10.1016/S0034-4257\(98\)00031-5](https://doi.org/10.1016/S0034-4257(98)00031-5).
579

580 IASOA, 2018: International Arctic Systems for Observing the Atmosphere. Accessed 21 May
581 2018, <https://www.esrl.noaa.gov/psd/iasoa/>.
582

583 IPCC, 2013: Climate Change 2013: The Physical Science Basis. Contribution of Working
584 Group I to the Fifth Assessment Report of the Intergovernmental Panel on Climate Change,
585 [Stocker, T.F., D. Qin, G.-K. Plattner, M. Tignor, S.K. Allen, J. Boschung, A. Nauels, Y. Xia, V.
586 Bex and P.M. Midgley (eds.)]. Cambridge University Press, Cambridge, United Kingdom and
587 New York, NY, USA, 1535 pp, doi:10.1017/CBO9781107415324.
588

589 Kahn, R.A. and Coauthors, 2004: Aerosol data sources and their roles within PARAGON, *Bull.*
590 *Amer. Meteor. Soc.*, **85**, 1155-1122, <https://doi.org/10.1175/BAMS-85-10-1511>.
591

592 Kahn, R.A. and Coauthors, 2017: SAM-CAAM: A Concept for Acquiring Systematic Aircraft
593 Measurements to Characterize Aerosol Air Masses, *Bull. Amer. Meteor. Soc.*, **98**, 2215-2228,
594 <https://doi.org/10.1175/BAMS-D-16-0003.1>.
595

596 Kassianov, E. and Coauthors, 2017: Large Contribution of Coarse Mode to Aerosol
597 Microphysical and Optical Properties: Evidence from Ground-Based Observations of a
598 Transpacific Dust Outbreak at a High-Elevation North American Site, *J. Atmos. Sci.*, **74**, 1431-
599 1443, <https://doi.org/10.1175/JAS-D-16-0256.1>.
600

601 Kinne, S., and Coauthors, 2006: An AeroCom initial assessment – optical properties in aerosol
602 component modules of global models, *Atmos. Chem. Phys.*, **6**, 1815–1834, doi:10.5194/acp-6-
603 1815-2006.

604

605 Kulmala M., and Coauthors, 2011: General overview: European Integrated project on Aerosol
606 Cloud Climate and Air Quality interactions (EUCAARI) – integrating aerosol research from
607 nano to global scales, *Atmos. Chem. Phys.*, **11**, 13061–13143, [https://doi.org/10.5194/acp-11-](https://doi.org/10.5194/acp-11-13061-2011)
608 13061-2011.

609

610 Laj, P., and Coauthors, 2009: Measuring atmospheric composition change, *Atmos. Environ.*, **43**,
611 5351-5414, doi:10.1016/j.atmosenv.2009.08.020.

612

613 Lim, S., Lee, M., Lee, G., Kim, S., Kang, K., 2012: Ionic and carbonaceous compositions of
614 PM10, PM2.5 and PM1.0 at Gosan ABC Superstation and their ratios as source signature,"
615 *Atmos. Chem. Phys.*, **12**, 2007-2024, <https://doi.org/10.5194/acp-12-2007-2012>.

616

617 Lund Myhre, C. and Baltensperger, U., 2012: Recommendations for a Composite Surface-Based
618 Aerosol Network, WMO/GAW Report 207, World Meteorological Organization, Geneva,
619 http://library.wmo.int/pmb_ged/gaw_207.pdf.

620

621 Mann, G.W. and Coauthors, 2014: Intercomparison and evaluation of global aerosol
622 microphysical properties among AeroCom models of a range of complexity, *Atmos. Chem.*
623 *Phys.*, **14**, 4679–4713, doi:10.5194/acp-14-4679-2014.

624

625 Matsui, H. and Coauthors, 2013: Spatial and temporal variations of new particle formation in
626 East Asia using an NPF-explicit WRF-chem model: North-south contrast in new particle
627 formation frequency, *J. Geophys. Res.*, **118**, 11647–11663, doi:10.1002/jgrd.50821.

628

629 Mueller, T. and Coauthors, 2011a: Characterization and intercomparison of aerosol absorption
630 photometers: result of two intercomparison workshops, *Atmos. Meas. Tech.*, 4, 245-268,
631 doi:10.5194/amt-4-245-2011.

632

633 Mueller, T., Laborde, M., Kassel, G., and Wiedensohler, A., 2011b: Design and performance of
634 a three-wavelength LED-based total scatter and backscatter integrating nephelometer, *Atmos.*
635 *Meas. Tech.*, 4, 1291-1303, doi:10.5194/amt-4-1291-2011.

636

637 NILU, 2018: EMEP: Hosting the GAW WDCA, Accessed 21 May 2018, <http://ebas.nilu.no/>.

638

639 NOAA, 2018a: Network publications. Accessed 21 May 2018,
640 <ftp://aftp.cmdl.noaa.gov/aerosol/doc/newsletter/publications.html>.

641

642 NOAA, 2018b: ESRL/GMD Aerosol Measurements. Accessed 21 May 2018,
643 <https://www.esrl.noaa.gov/gmd/aero/instrumentation/instrum.html>.

644

645 NOAA, 2018c: Aerosol System Inlet. Accessed 21 May 2018,
646 https://www.esrl.noaa.gov/gmd/aero/instrumentation/inlet_system.html.

647

648 NOAA, 2018d: CPD3 loggable instruments. Accessed 21 May 2018,
649 https://www.esrl.noaa.gov/gmd/instrumentation/cpd_inst.html

650

651 Ogren, J.A., 1995: A systematic approach to in-situ observation of aerosol properties, In:
652 *Aerosol Forcing of Climate*, eds. R. Charlson and J. Heintzenberg, John Wiley & Sons, Ltd.,
653 215-226.

654

655 Ogren, J.A., Wendell, J., Andrews, E., and Sheridan, P., 2017: Continuous light absorption
656 photometer for long-term studies, *Atmos. Meas. Tech.*, **10**, 4805-4818,
657 <https://doi.org/10.5194/amt-10-4805-2017>.

658

659 Pahlow, M. and Coauthors, 2006: Comparison between lidar and nephelometer measurements of
660 aerosol hygroscopicity at the Southern Great Plains Atmospheric Radiation Measurement site, *J.*
661 *Geophys. Res.*, **111**, doi:10.1029/2004JD005646.

662

663 Pandolfi, M. and Coauthors, 2018: A European aerosol phenomenology-6: Scattering properties
664 of atmospheric aerosol particles from 28 ACTRIS sites, *Atmos. Chem. Phys.*, **18**, 7877-7911,
665 <https://doi.org/10.5194/acp-18-7877-2018>.

666

667 Perry, K.D., Cahill, T.A., Schnell, R.C., and Harris, J.M., 1999: Long-range transport of
668 anthropogenic aerosols to the National Oceanic and Atmospheric Administration baseline station

669 at Mauna Loa Observatory, Hawaii, *J. Geophys. Res.*, **104**, 18521-18533,
670 doi:10.1029/1998JD100083.
671
672 PSI, 2018: CATCOS Aerosol Measurements. Accessed 21 May 2018,
673 <https://www.psi.ch/catcos/>.
674
675 Quinn P. K., Miller, T. L., Bates, T. S., Ogren, J. A., Andrews, E., and Shaw, G. E., 2002: A 3-
676 year record of simultaneously measured aerosol chemical and optical properties at Barrow,
677 Alaska, *J. Geophys. Res.*, **107**, doi:10.1029/2001JD001248.
678
679 Rivera, H., Ogren, J.A., Andrews, E., Mayol-Bracero, O.L., 2017: Variations in the
680 physicochemical and optical properties of natural aerosols in Puerto Rico – Implications for
681 climate, *Atmos. Chem. Phys. Disc.*, in review, <https://doi.org/10.5194/acp-2017-703>.
682
683 Schmeisser, L., and Coauthors, 2017: Classifying aerosol type using in-situ surface spectral
684 aerosol optical properties, *Atmos. Chem. Phys.*, **17**, 12097-12120, [https://doi.org/10.5194/acp-17-](https://doi.org/10.5194/acp-17-12097-2017)
685 [12097-2017](https://doi.org/10.5194/acp-17-12097-2017).
686
687 Schmeisser, L., and Coauthors, 2018: Seasonality of aerosol optical properties in the Arctic,
688 *Atmos. Chem. Phys. Disc.*, in review, <https://www.atmos-chem-phys-discuss.net/acp-2017-1117..>
689
690 Sharma, N.C.P., Barnes, J.E., 2016: Boundary layer characteristics over a high altitude station,
691 Mauna Loa Observatory, *Aerosol Air Qual. Res.*, **16**, 729-737, doi:10.4209/aaqr.2015.05.0347.

692

693 Sharma, S., and Coauthors, 2017: An evaluation of three methods for measuring black carbon at
694 Alert, Canada, *Atmos. Chem. Phys. Discuss.*, **17**, <https://doi.org/10.5194/acp-2017-339>, in
695 review.

696

697 Sharma, S., Ishizawa, M, Chan, D., Lavoué, D., Andrews, E., Eleftheriadis, K and
698 Maksyutov, S., 2013: 16-year simulation of Arctic black carbon: transport, source contribution,
699 and sensitivity analysis on deposition, *J. Geophys. Res.*, **118**, doi:10.1029/2012JD017774.

700

701 Sheridan, P.J., Delene, D.J., and Ogren, J.A., 2001: Four years of continuous surface aerosol
702 measurements from the Department of Energy's Atmospheric Radiation Measurement Program
703 Southern Great Plains Cloud and Radiation Testbed site, *J. Geophys. Res.* **106**, 20735-20747,
704 doi:10.1029/2001JD000785.

705

706 Sheridan, P.J., Andrews, E., Ogren, J.A., Tackett, J., Winker, D.M., 2012: Vertical profiles of
707 aerosol optical properties over central Illinois and comparison with surface and satellite
708 measurements," *Atmos. Chem. Phys.*, 12, 11695-11721, doi: 10.5194/acp-12-11695-2012.

709

710 Sheridan, P.J., Andrews, E., Schmeisser, L., Vasel, B., and Ogren, J.A., 2016: Aerosol
711 Measurements at South Pole: Climatology and Impact of Local Contamination, *AAQR*, **16**, 855-
712 872, doi:10.4209/aaqr.2015.05.0358.

713

714 Sherman, J. P. and McComiskey, A., 2018: Measurement-based climatology of aerosol direct
715 radiative effect, its sensitivities, and uncertainties from a background southeast U.S. site, *Atmos.*
716 *Chem. Phys.*, **18**, 4131-4152, <https://doi.org/10.5194/acp-18-4131-2018>.
717

718 Sherman, J.P., Sheridan, P.J., Ogren, J.A., Andrews, E., Hageman, D.C., Schmeisser, L.,
719 Jefferson, A., and Sharma, S., 2015: A multi-year study of lower tropospheric aerosol variability
720 and systematic relationships from four North American regions, *Atmos. Chem. Phys.*, **15**, 12487-
721 12517, <https://doi.org/10.5194/acp-15-12487-2015>.
722

723 Shinozuka, Y., and Coauthors, 2015: The relationship between cloud condensation nuclei (CCN)
724 concentration and light extinction of dried particles: indications of underlying aerosol processes
725 and implications for satellite-based CCN estimates, *Atmos. Chem. Phys.*, **15**, 7585-7604,
726 <https://doi.org/10.5194/acp-15-7585-2015>.
727

728 Sinha, P.R. and Coauthors, 2017: Evaluation of ground-based black carbon measurements by
729 filter-based photometers at two Arctic sites, *J. Geophys. Res.*, **122**, 3544-3572,
730 [doi:10.1002/2016JD025843](https://doi.org/10.1002/2016JD025843).
731

732 Skeie, R.B, Berntsen, T., Myhre, G., Pedersen, J.A., Strom, J., Gerland, S., and Ogren, J.A.,
733 2011: Black carbon in the atmosphere and snow, from pre-industrial times until present, *Atmos.*
734 *Chem. Phys.*, **11**, 6809-6836, <https://doi.org/10.5194/acp-11-6809-2011>.
735

736 Sorribas, M., Andrews, E., Adame, J.A., Yela, M., 2017: An anomalous African dust event and
737 its impact on aerosol radiative forcing on the Southwest Atlantic coast of Europe in February
738 2016, *Sci. Tot. Environ.*, **583**, 269-279, <https://doi.org/10.1016/j.scitotenv.2017.01.064>.
739

740 Sorribas, M., Ogren, J.A., Olmo, F.J., Quirantes, A., Fraile, R., Gil-Ojeda, M., Alados-
741 Arboledas, L., 2015: Assessment of African desert dust episodes over the southwest Spain at sea
742 level using in situ aerosol optical and microphysical properties, *Tellus B*, **67**, doi:
743 <https://doi.org/10.3402/tellusb.v67.27482>.
744

745 Spracklen, D. V., and Coauthors, 2010: Explaining global surface aerosol number concentrations
746 in terms of primary emissions and particle formation, *Atmos. Chem. Phys.*, **10**, 4775-4793,
747 <https://doi.org/10.5194/acp-11-10661-2011>.
748

749 Stone, R.S., Anderson, G.P., Andrews, E., Dutton, E.G., and Shettle, E.P., 2007: Incursions and
750 radiative impact of Asian dust in northern Alaska, *Geophys. Res. Lett.*, **34**,
751 doi:10.1029/2007GL029878 .
752

753 Titos, G. and Coauthors, 2017: Spatial and temporal variability of carbonaceous aerosols:
754 Assessing the impact of biomass burning in the urban environment, *Sci. Tot. Environ.*, **578**, 613-
755 625, doi:10.1016/j.scitotenv.2016.11.007.
756
757

758 Uttal T., and Coauthors, 2016: International Arctic Systems for Observing the Atmosphere: An
759 International Polar Year Legacy Consortium, *Bull. Amer. Meteor. Soc.*, **97**, 1033-1056,
760 <https://doi.org/10.1175/BAMS-D-14-00145.1>.
761

762 Wang, R., and Coauthors, 2018: Representativeness error in the ground-level observation
763 networks for black carbon radiation absorption, *Geophys. Res. Lett.*, doi:10.1002/2017GL076817.
764

765 WCCAP, 2018: World Calibration Centre for Aerosol Physics, Accessed 21 May 2018,
766 <http://www.wmo-gaw-wcc-aerosol-physics.org>.
767

768 Wiedensohler, A., and Coauthors, 2012: Mobility particle size spectrometers: harmonization of
769 technical standards and data structure to facilitate high quality long-term observations of
770 atmospheric particle number size distributions, *Atmos. Meas. Tech.*, **5**, 657-685,
771 doi:10.5194/amt-5-657-2012.
772

773 Wilcox, J.D., 1956: Isokinetic Flow and Sampling, *J. Air Poll. Contr. Assoc.*, **5**, 226-245, doi:
774 10.1080/00966665.1956.10467715
775

776 WMO, 2011: WMO/GAW Standard Operating Procedures for In-situ Measurements of Aerosol
777 Mass Concentration, Light Scattering and Light Absorption, GAW Report No. 200, World
778 Meteorological Organization, Geneva, http://library.wmo.int/pmb_ged/gaw_200.pdf.
779

780 WMO, 2016: WMO/GAW Aerosol Measurement Procedures, Guidelines, and
781 Recommendations, GAW Report No. 227, World Meteorological Organization, Geneva,
782 https://library.wmo.int/opac/doc_num.php?explnum_id=3073.
783
784 WMO, 2018: Low-cost sensors for the measurement of atmospheric composition: overview of
785 topic and future applications, WMO Report No. 1215, World Meteorological Organization,
786 Geneva,
787 https://www.wmo.int/pages/prog/arep/gaw/documents/Low_cost_sensors_post_review_final.pdf.
788
789 Yu, F. and Hallar, A.G., 2014: Difference in particle formation at a mountaintop location during
790 spring and summer: implications for the role of sulfuric acid and organics in nucleation, *J.*
791 *Geophys. Res.*, **119**, 12246-12255, doi:10.1002/2014JD022136.
792
793 Zanatta, M. and Coauthors, 2016: A European aerosol phenomenology-5: Climatology of black
794 carbon optical properties at 9 regional background sites across Europe, *Atmos. Environ.*, **145**,
795 346-364, <http://dx.doi.org/10.1016/j.atmosenv.2016.09.035>.
796

797 **Table 1. Description of aerosol parameters mentioned in text**

Aerosol Parameter (symbol)	Description of parameter and measurement instrument or equation for calculating
Aerosol Light Scattering (σ_{sp})	Indicator of aerosol amount and related optical effects. Measured in the FAN with an integrating nephelometer.
Aerosol Light Absorption (σ_{ap})	Indicator of particle darkness; related to black carbon (BC). Measured in the FAN with a filter-based absorption photometer.
Aerosol Number Concentration (N)	Indicator of local contamination; precursor of cloud condensation nuclei. Measured in the FAN with a condensation particle counter.
Scattering Ångström exponent (SAE)	SAE describes the wavelength-dependence of scattered light. When scattering is dominated by sub-micrometer particles the SAE values are typically around 2, while SAE values closer to 0 occur when the scattering is dominated by particles larger than a few micrometers in diameter. SAE = $-\log[\sigma_{sp}(\lambda_1)/\sigma_{sp}(\lambda_2)]/\log(\lambda_2/\lambda_1)$
Single-scattering albedo (SSA)	SSA describes the relative contributions of scattering and absorption to the total light extinction. Purely scattering aerosols (e.g., sulfuric acid) have SSA values of 1, while very strong absorbers (e.g., elemental carbon) have SSA values around 0.3. SSA = $\sigma_{sp}/(\sigma_{sp} + \sigma_{ap})$

798

799 **Figure Captions**

800

801 Figure 1. Map of current and former long-term sites in FAN network superimposed on a
802 nighttime lights image (Credit: NASA Earth Observatory/NOAA NGDC). Former sites RSL,
803 SGP and WSA were FAN collaborations, while THD and SMO were solely NOAA
804 observations.

805

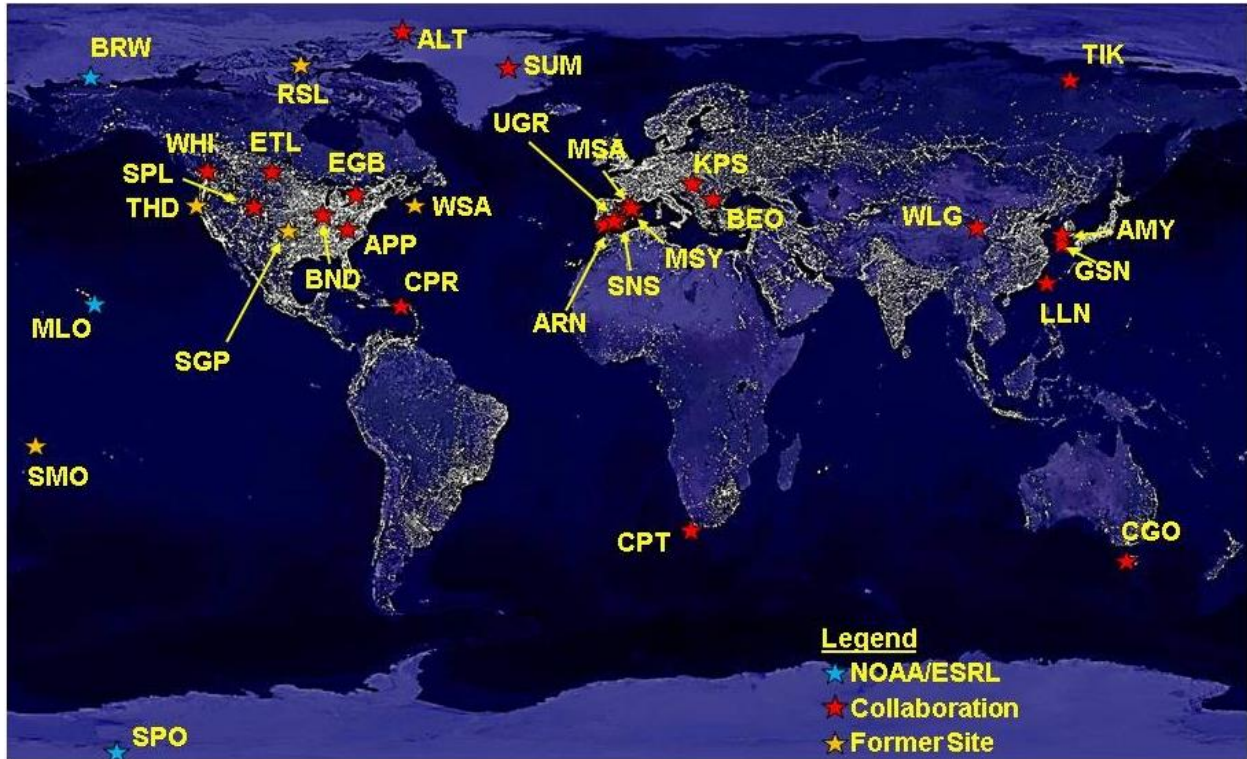
806 Figure 2. Annual aerosol climatology for long-term sites in network. Stations are ordered by
807 increasing scattering coefficient. (a) scattering coefficient; (b) absorption coefficient; (c)
808 scattering Ångström exponent (d) single-scattering albedo. Scattering and absorption have units
809 of Mm^{-1} , scattering Ångström exponent and single-scattering albedo are unitless. Values are
810 reported at 550 nm, scattering Ångström exponent is calculated for the blue/green wavelength
811 pair. Whiskers represent 5th and 95th percentiles, edges of box are 25th and 75th percentiles and
812 midpoint line in box is median value of annual climatology. Blue indicates NOAA observatories,
813 red indicates collaborator sites. Some sites are not shown due little available data (e.g., less than
814 a year of data available or data not yet being QC'd).

815

816 Figure 3. Long-term climatology of aerosol light scattering (at 550 nm) in units of Mm^{-1} at
817 Bondville. (a) monthly variability as function of year; (b) diurnal variability as function of month
818 (thick black horizontal line indicates local noon). Both plots are based on data obtained from
819 1995 through 2016.

820

821



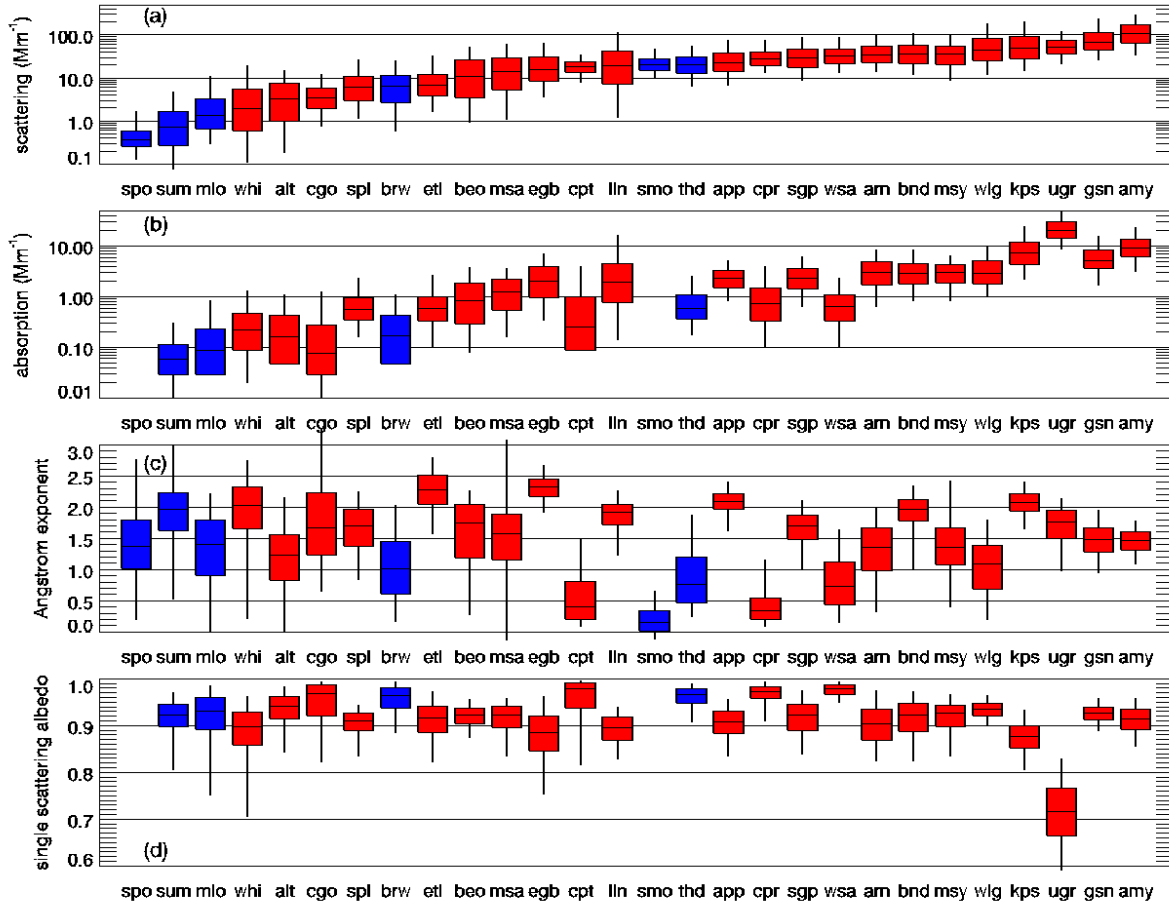
822

823 Figure 1. Map of current and former long-term sites in FAN network superimposed on a

824 nighttime lights image (Credit: NASA Earth Observatory/NOAA NGDC). Former sites RSL,

825 SGP and WSA were FAN collaborations, while THD and SMO were solely NOAA

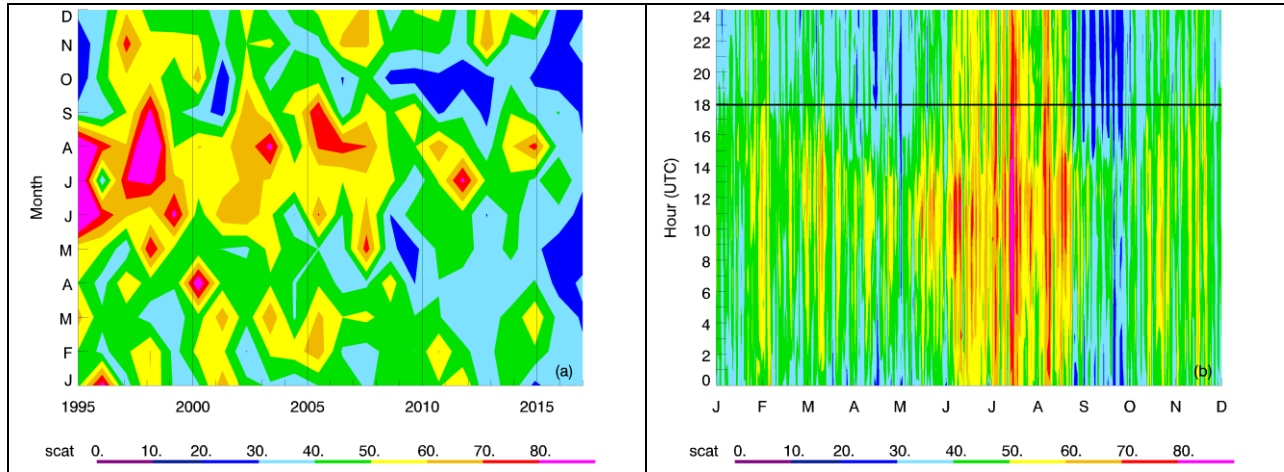
826 observations.



827
 828 Figure 2. Annual aerosol climatology for long-term sites in network. Stations are ordered by
 829 increasing scattering coefficient. (a) scattering coefficient; (b) absorption coefficient; (c)
 830 scattering Ångström exponent (d) single-scattering albedo. Scattering and absorption have units
 831 of Mm^{-1} , scattering Ångström exponent and single-scattering albedo are unitless. Values are
 832 calculated from daily averages reported at (or adjusted to) 550 nm, scattering Ångström exponent
 833 is calculated for the blue/green wavelength pair. Whiskers represent 5th and 95th percentiles,
 834 edges of box are 25th and 75th percentiles and midpoint line in box is median value of annual
 835 climatology. Blue indicates NOAA observatories, red indicates collaborator sites. Some sites are
 836 not shown due to little available data (e.g., less than a year of data available or data not yet being
 837 QC'd).

838

839



840

841 Figure 3. Long-term climatology of aerosol light scattering (at 550 nm) in units of Mm^{-1} at
842 Bondville. (a) monthly variability as function of year; (b) diurnal variability as function of month
843 (thick black horizontal line indicates local noon). Both plots are based on data obtained from
844 1995 through 2016.